Article

Acid resistance of lightweight brick powder based alkali activated material from construction and demolition wastes

Kai Tai Wan[1,2†,‡]*, Amende Sivanathan [1,‡] Gediminas Kastiukas [1] and Xiangming Zhou [1]

[1] Department of Civil and Environmental Engineering, Brunel University London, UK
[2] Experimental Technology Centre, Brunel University London, UK
* Correspondence: KaiTai.Wan@brunel.ac.uk; Tel.: +44-1895-265-476
† Current address: Brunel University London, Uxbridge, Middlesex, UB8 3PH, UK
‡ These authors contributed equally to this work.

Abstract: The annual construction and demolition waste (CDW) generated from EU construction sector was 850 million tons, which represented 31% of the total waste generation and about 28% of CDW was ceramics (bricks and tiles). In this study, the feasibility of using CDW brick powder as the precursor of alkali activated mortar (AAM) and extruded polystyrene (XPS) as the lightweight aggregates to form lightweight brick powder AAM (LW-BP-AAM) for non-structural applications was investigated. The thermal conductivity of LP-BPAAM was 0.112 W/m·K with density of about 1,135 kg/m^3 which was lower than the counterparts with similar density in literature. The acid resistance of LW-BP-AAM is comparable to conventional fly ash based AAM and superior than ordinary Portland cement. From the scanning electron microscopy with energy dispersive X-ray spectroscopy, there was no severe damage on the surface of LW-BP-AAM but aluminate was removed from the matrix which was further verified in Fourier transform infrared spectroscopy. The mass and strength loss of LP-BP-AAM was 1.5% and 33%, respectively. Although the compressive strength of the LP-BP-AAM was low (about 1.8 MPa), it can be improved by optimising the particle size of the XPS aggregates.

Keywords: alkali activated materials; construction and demolition waste; brick powder; acid resistance; extruded polystyrene aggregates lightweight materials

1. Introduction

The rapid growth of the construction industry worldwide during the past decades has resulted tremendous volume of construction and demolition waste (CDW) and it has constituted the largest single waste stream within the European Union (EU). CDW is generated from construction, renovation, rehabilitation and demolition of buildings and infrastructures. The composition of CDW varies from different activities and structures, but in general, they are bulky and heavy materials, such as concrete, wood, asphalt, gypsum, metals, bricks, glass, expanded polystyrene (EPS) and extruded polystyrene (XPS), that are mainly disposed to landfill. The annual CDW generated from EU construction sector was 850 million tons, which represented 31% of the total waste generation [1] and about 28% of CDW was ceramics (bricks and tiles) [2]. Construction of new buildings alone, generates an average of 39 kg of construction waste per square metre of a building.

Brick is widely used for curtain walls and partition walls of buildings. EPS and XPS are widely used on building envelop to enhance thermal insulation and energy efficiency of buildings. There were different ways of using recycled brick powder in previous research such as used as fine and coarse aggregates in concrete [3,4] , cement replacement [5–7] and the precursor of geopolymer [8,9], which is a sub-group of alkali-activated material (AAM). The recycled EPS was mainly used as the aggregates for lightweight concrete [10–12].

Table 1. Chemical composition (% mass) of PLC, FA and BP-CDW from XRF measurement.

	PLC	FA	BP-CDW
SiO_2	17.5	57.5	69.5
CaO	68.9	3.8	0.3
Al_2O_3	4.9	25.6	16.6
Fe_2O_3	3.1	10.2	6.9
MgO	1.3	2.0	2.0
TiO_2	0.4	1.0	0.9
Na_2O	0.2	1.2	0.2
K_2O	0.6	2.8	2.8
SO_3	2.6	–	–
LOI	–	–	–

In this study, the feasibility of using brick powder from CDW as the precursor of AAM as the binder and XPS from CDW as the lightweight aggregates to recycle brick from CDW to form brick-like material for non-structural applications as conventional lightweight brick was investigated. In order to evaluate the quality and stability of the chemical product, in addition to test the mechanical strength, instead of indirect probing by different material characterisation techniques [13,14], the acid resistance test of the proposed material was measured and compared with conventional blended cement [15] and fly ash based AAM [16] since ordinary Portland cement (OPC) based concrete is prone to acid attack while the acid resistance of geopolymer is intrinsically superior than OPC.

2. Detail of experiments

2.1. Materials and chemicals

The materials used in this study were Portland limestone cement (PLC), fly ash (FA), brick powder from construction and demolition waste (BP-CDW), sharp sand and extruded polystyrene from construction and demolition waste (XPS-CDW). The PLC used in this experimental programme followed BS EN 197-1 – CEM II/A-L 32,5 R (Rugby Premium Cement, CEMEX UK). The FA used in this study was from coal-fired power plant followed BS EN 197-1 (CEMEX UK). The BP-CDW was obtained from the the disposed brick, which could not pass the quality assurance process in a brick manufacturing factory (NRGIA, Poland). The chemical compositions from X-ray fluorescence (XRF) of PLC, FA and BP-CDW are shown in Table 1. The disposed brick was crushed into sand-size particle in the factory and then ground in a planetary ball mill in laboratory (PM 100, RETSCH). The particle size distribution of the milled BP-CDW (BP-CDW-M) under 500 rpm for 20 minutes measured by a particle size analyser (Malvern Mastersizer 2000) is shown in Figure 1. The specific surface area and surface weighted mean particle size was 51.9 m^2/g and 0.127 μm, respectively. The micrographs of PLC, FA and BP-CDW-M are shown in Figure 2. The shape of both PLC and BP-CDW-M is irregular while FA is spherical. The XPS-CDW was cut (NRGIA, Poland) to the particle size about 1 to 2 mm.

The alkali activating solution was made of sodium hydroxide pearl (NaOH) (98% purity, Fisher Scientific UK), potassium hydroxide pellet (KOH) (98% purity, Sigma Aldrich, UK), sodium silicate solution (Na_2SiO_3) (technical grade, d=1.5, Fisher Scientific, UK) and colloidal silicon dioxide (SiO_2) (50% wt in H_2O, Sigma Aldrich, UK). The acidic bath for acid resistance test was prepared from sulfuric acid (95-98% w/w, Fisher Scientific, UK).

2.2. Preparation alkali activating solution

2.2.1. Alkali activating solution for the fly ash based alkali activated mortar

The alkali activating solution for the FA based alkali activated mortar (AAS-FA) consisted of 8 M sodium hydroxide solution mixed with as-received sodium silicate solution in the mass ratio of 1:1.22.

Preprints (www.preprints.org) | NOT PEER-REVIEWED | Posted: 25 June 2018 doi:10.20944/preprints201806.0387.v1

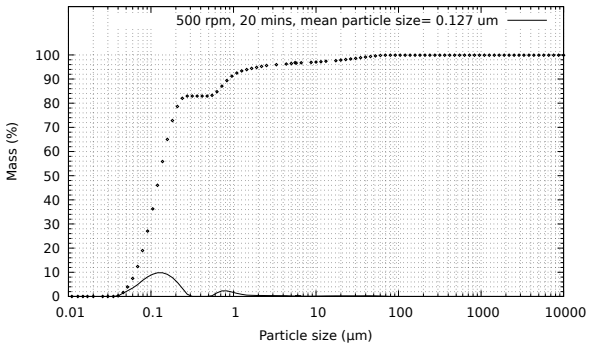

Figure 1. Particle size distribution and cumulative particle size distribution of BP-CDW.

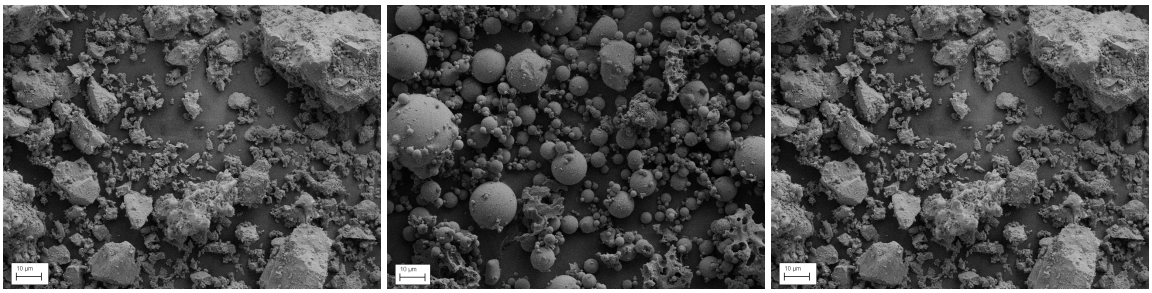

(a) PLC **(b)** FA **(c)** BP-CDW-M

Figure 2. Micrographs of the raw materials. (a) PLC, (b) FA and (c) BP-CDW-M.

The mix proportion in mass of AAS-FA is shown in Table 2. To prepare 1 L 8 M sodium hydroxide solution, 320 g NaOH was added to 750 mL deionised water first and mixed by a magnetic stirrer for 12 hours until the temperature was in equilibrium to the ambient. Then, the solution was transferred to a volumetric flask and extra deionised water was added to 1 L volume.

2.2.2. Alkali activating solution for the lightweight brick powder based alkali activated mortar

The alkali activating solution for the lightweight BP-CDW-M based alkali-activated mortar (AAS-BP) consisted of NaOH, KOH and SiO_2 colloidal solution and the mix proportion is shown in Table 2. To prepare AAS-BP, NaOH and KOH was dissolved in deionised water in a beaker covered by cling film to prevent evaporation and mixed by magnetic stirrer. Followed from the complete dissolution of NaOH and KOH, SiO_2 colloidal solution was added and it could be mixed thoroughly from the elevated temperature induced by the exothermic dissolution of NaOH and KOH. The final AAS-BP was a gel-like solution and it was used for sample preparation immediately after cooled down to ambient.

Table 2. Mix proportion of alkali activating solution in mass ratio.

	NaOH	KOH	Na_2SiO_3	SiO_2	Deionised water
AAS-FA	1.00	–	5.03	–	3.13
AAS-BP	1.00	1.40	–	3.00	3.88

Preprints (www.preprints.org) | NOT PEER-REVIEWED | Posted: 25 June 2018 doi:10.20944/preprints201806.0387.v1

2.2.3. 5% sulfuric acid bath

To prepare 1 L 5% sulfuric acid bath, 51.8 mL H_2SO_4 solution was added to 750 mL deionised water in a volumetric flask first and extra extra deionised water was added up to 1 L after the temperature of the solution was in equivalent to the ambient. The pH of the 5% acid bath was 0.32.

2.3. Sample preparation

2.3.1. PLC samples

Twelve 100 mm × 100 mm × 100 mm PLC mortar samples were prepared in a desktop Hobart mixer. The mix proportion of PLC to water to sand used in this study was 1 : 0.45 : 0.30. The cast samples were covered by cling film at room temperature for 24 hours and then demoulded followed by water curing at room temperature for further 28 days.

2.3.2. FA-AAM samples

Twelve 100 mm × 100 mm × 100 mm FA based alkali activated mortar (FA-AAM) samples were prepared with the mix proportion of FA to AAS-FA to sand to be 1 : 0.45 : 0.3. FA and sand was dry mixed in a desktop Hobart mixer at the lowest speed for 5 minutes and then AAS-FA was added to form a homogeneous paste. The cast samples were covered by cling film and then immediately thermal-cured at 80° for 48 hours. After thermal-curing, the samples were demoulded and air-cured at room temperature for 12 days before testing.

2.3.3. LW-BP-AAM samples

Fifteen 100 mm × 100 mm × 100 mm lightweight BP-CDW-M alkali activated mortar (LW-BP-CDW-M-AAM) samples (12 for acid resistance test and 3 for thermal conductivity test) were prepared with mix proportion of BP-CDW-M to AAS-BP to XPS-CDW to be 1 : 0.53 : 0.03. BP-CDW-M was mixed with AAS-BP at the lowest speed in a desktop Hobart mixer for 5 minutes to form homogeneous paste. Then, XPS-CDW was added and further mixed for 2 minutes. The cast samples were covered by cling film and cured at room temperature for 2 hours followed by thermal-curing at 80° for 48 hours. After thermal-curing, the samples were demoulded and air-cured at room temperature for 12 days before testing.

2.4. Testing

2.4.1. Acid resistance test

The FA-AAM and LW-BP-AAM samples were put in water bath for 4 days after air-curing to saturate the samples. Before the acid resistance test, all 36 PLC, FA-AAM and LW-BP-AAM samples were wiped by a damped towel to induce saturated surface condition (SSD) to prevent sorption and then the initial mass was measured. Then, the compressive strength of 3 samples of each type was measured. During the test, nine samples of each type were immersed into the prepared 5% sulfuric acid bath in three separated containers to prevent cross-contamination. The mass of 3 samples of each type at the 7th, 14th and 28th day was measured at SSD condition by washing the sample with tap water and wiped dry by a damped towel followed by mass and compressive strength measurement. Images of the samples before and after the acid resistance test were taken by a high resolution camera to qualitatively observe the degradation after 7, 14 and 28 days in 5% sulfuric acid bath. The mass of the samples in SSD was measured in an electronic balance with precision of 1 g. The compressive strength of PLC, FA-AAM and LW-BP-AAM before and after acid resistance test was measured by a concrete crusher with loading rate of 1.5 kN/s [17]. The pH of the acid bath was measured weekly. If there was significant change in pH in the acid bath, it was replaced by fresh acid bath. The relative mass (m_f / m_i) and relative strength (σ_c^f / σ_c^i) can be estimated where m_i, m_f, σ_c^i and σ_c^f are the mass just

 doi:10.20944/preprints201806.0387.v1

before the test, mass after the test, compressive strength before the test and the compressive strength after the test, respectively.

2.4.2. Material characterisation

The morphology of the sample after compression test of each type of samples before and after the exposure in acid bath for 28 days was observed under scanning electron microscope (LEO 1455VP). The samples were sputtered with a gold coating for 45 seconds in a sputter coater (Polaron-SC7640). Elemental analysis was performed by energy dispersive X-ray spectroscopy (EDX) to study the change of chemical composition.

The absorption spectra of the material collected from the central core and the outer surface of all samples after compressive test was measured by Fourier transform infrared spectroscopy (FTIR, Perkin Elmer spectrum One) in order to observe the change in chemical bonding before and after the acid resistance test. Each spectrum was scanned from 4000 cm^{-1} to 600 cm^{-1} with 8 cm^{-1} resolution for 32 scans each.

2.4.3. Thermal conductivity

The coefficient of thermal conductivity of LW-BP-AAM was measured by a heat flow metre (TA Instruments FOX200). The samples of LW-BP-AAM were cut to 100 mm$\times$100 mm$\times$18 mm. The temperatures of the hot and cold plate were set at 20° and 0°, respectively.

3. Results and discussions

3.1. Acid resistance test

The averaged densities of PLC, FA-AAM and LW-BP-AAM samples before the acid resistance test were 2,170 kg/m^3, 1,896 kg/m^3 and 1,135 kg/m^3, respectively. The averaged compressive strengths of PLC, FA-AAM and LW-BP-AAM samples before the acid resistance test were 38.2 MPa, 24.2 MPa and 1.76 MPa, respectively. The compressive strength of LW-BP-AAM was lower than other lightweight counterpart with EPS as the lightweight aggregates [18] but it was better than the aerated counterpart [19,20]. The compressive strength of LW-BP-AAM can be optimised with different particle size of XPS-CDW. Since XPS-CDW is from waste, the only cost is the basic cleaning and grinding.

Figure 3 shows the relative mass of PLC, FA-AAM and LW-BP-AAM after the acid resistance test. The mass loss of PLC after 28 days in 5% sulfuric acid was 9.5% while that of FA-AAM and LW-BP-AAM was only about 1.5%. It was consistent with the visual inspection of the appearance of the sample after the acid resistance test as in Figure 4. There was no significant change on the surface appearance after cleaning of FA-AAM and LW-BP-AAM. However, the surface of PLC sample was etched and white gel was deposited on the surface (Figure 5) which was the reaction product between the sulfuric acid and the calcium content in PLC sample. Figure 6 shows the relative strength of the samples after the acid resistance test. The strength loss of PLC (14%) and FA-AAM (17%) at the 7th day was similar while that of LW-BP-AAM was 28%. At the 14th day in the acid bath, the strength loss of PLC, FA-AAM and LW-BP-AAM was 39%, 24% and 30%, respectively. At the 28th day in the acid bath, the strength loss of PLC, FA-AAM and LW-BP-AAM was 66%, 34% and 33%, respectively. Although the strength loss of LW-BP-AAM was significant in the first 7 days, the strength loss was stabilised and comparable with FA-AAM at the 28th days. It can be verified and explained from the material characterisation.

Preprints (www.preprints.org) | NOT PEER-REVIEWED | Posted: 25 June 2018 doi:10.20944/preprints201806.0387.v1

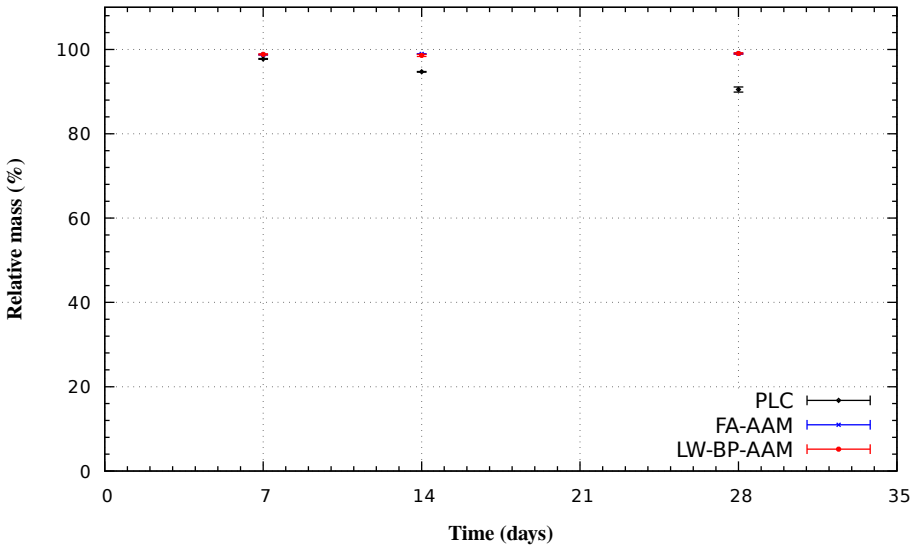

Figure 3. Relative mass of acid resistance test.

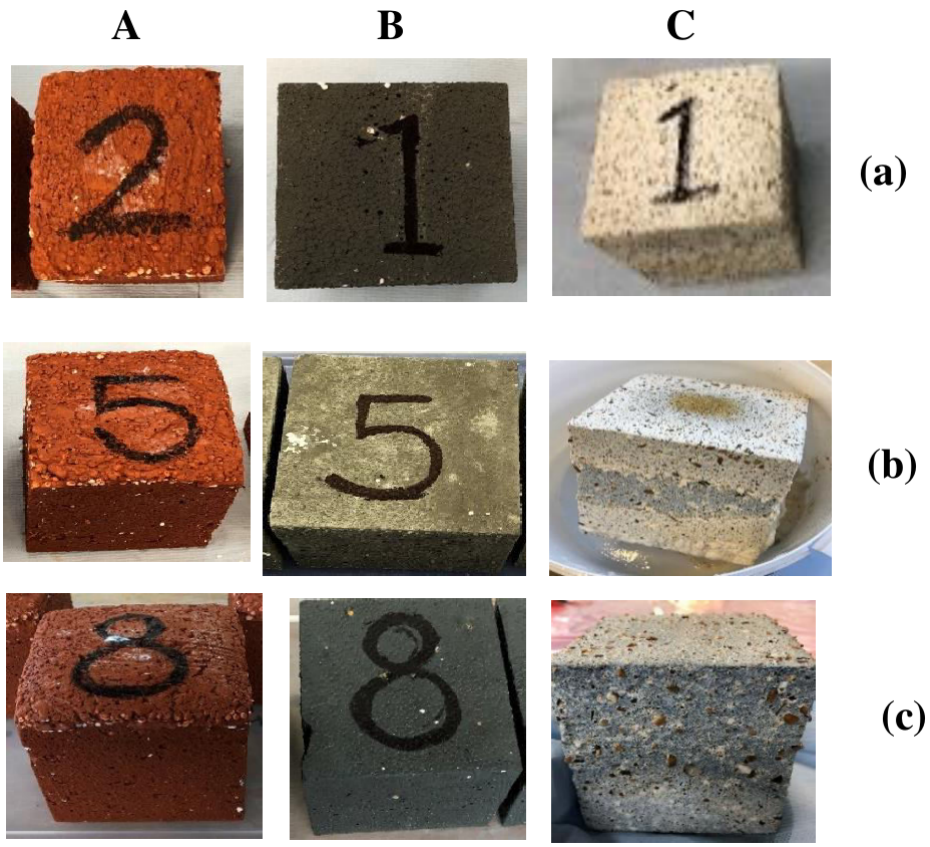

Figure 4. Visual inspection of the samples after acid resistance test. A: LW-BP-AAM, B: FA-AAM, C: PLC, (a) 7 days, (b) 14 days and (c) 28 days.

Preprints (www.preprints.org) | NOT PEER-REVIEWED | Posted: 25 June 2018 doi:10.20944/preprints201806.0387.v1

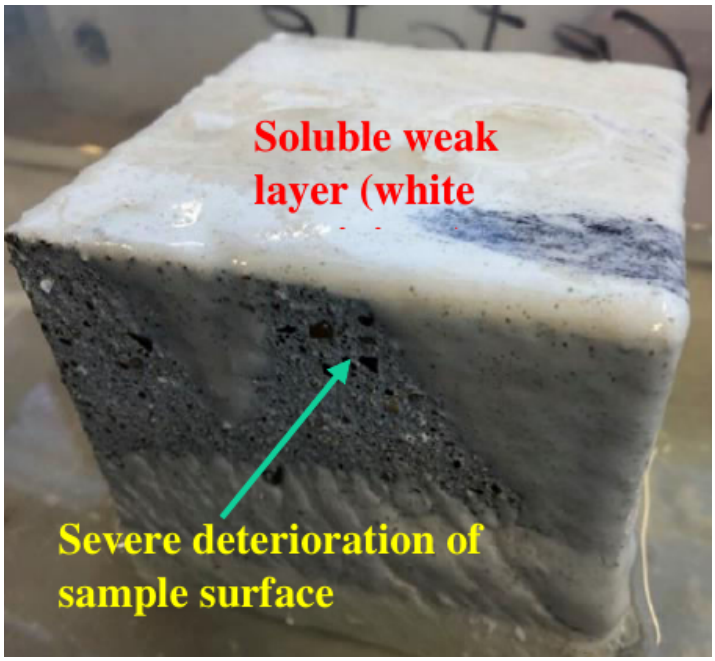

Figure 5. Visual inspection of the PLC sample after immersing in 5% sulfuric acid bath for 28 days before cleaning.

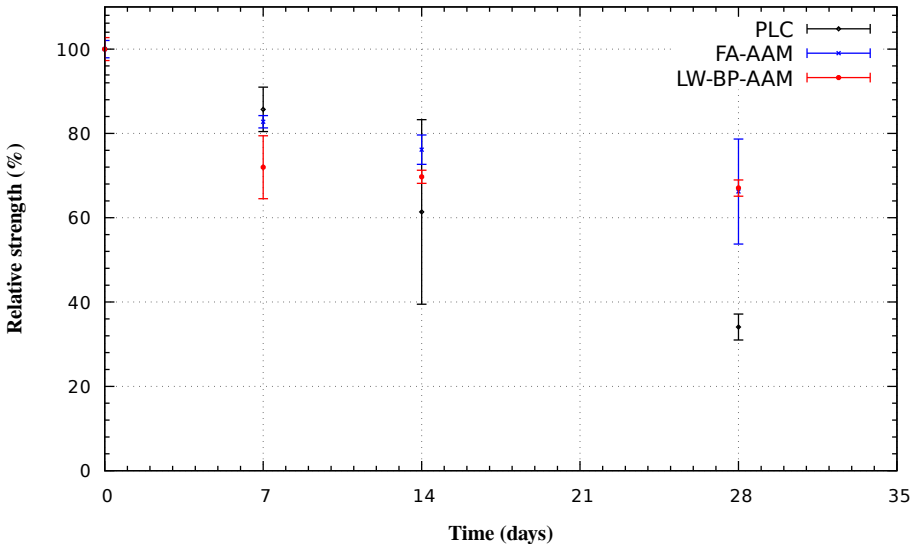

Figure 6. Relative strength of PLC, FA-AAM and LW-BP-AAM after acid resistance test.

3.2. Materials characterisation

3.2.1. SEM/EDX

Figure 7 shows the micrographs of the samples taken near the surface before and after the acid resistance test for 28 days. The microstructure of PLC sample before the acid resistance test was dense (Figure 7a). After the acid resistance test, large pores were observed (Figure 7b) which was possibly due to the dissolution of Portlandite and it explained why the compressive strength of PLC decreased significantly (66%) after the immersing in 5% sulfuric acid bath for 28 days. Figure 7c shows the dense matrix of FA-AAM before the acid resistance test. After the acid resistance test for 28 days,

 doi:10.20944/preprints201806.0387.v1

Table 3. Results of SEM/EDX of FA-AAM and LM-BP-AAM before and after the acid resistance test for 28 days.

Elements	FA-AAM		LW-BP-AAM	
(wt%)	Before	After	Before	After
Si	31.26	47.28	29.24	44.79
Al	6.87	3.52	12.33	4.31
Ca	0.76	0	7.14	1.15
Na	5.77	0.27	7.97	0.12
Fe	1.56	1.13	2.59	4.21
S	0	0.53	0	5.65

there were microcracks observed in the matrix (Figure 7d). However, there was no large pore formed in the matrix in FA-AAM as the PLC samples. There was similar observation of the LW-BP-AAM samples (Figures 7e and 7f). From the EDX results in Table 3, the Si/Al mass ratio to be 4.55, which was equivalent to the molar ratio of 4.37 before the acid resistance test. After the FA-AAM was exposed to 5% sulfuric acid for 28 days, the Si/Al mass ratio was increased to 13.43, which was equivalent to molar ratio of 12.90. Similarly, the Si/Al mass ratio of LW-BP-AAM was increased from 2.37 before the acid resistance test to 10.39 after the test. The main reason was because of the dissolution of aluminate in acidic environment [21] and it could be verified from the FTIR spectra.

3.2.2. FTIR

Figure 8 shows the FTIR spectra of centre part and outer surface of FA-AAM and LW-BP-AAM samples before the acid resistance test as well as after immersing in 5% sulfuric acid for 7, 14 and 28 days. From the FTIR spectra taken from the outer surface of the FA-AAM samples (Figure 8a), the main peak at 995 cm^{-1}, which was corresponding to asymmetric stretching to Si-O-T (T = Si or Al) bond [22–24], before the acid resistance test was shifted to 1057, 1056 and 1049 cm^{-1} after 7, 14 and 28 days, respectively. For the samples taken from the centre part of FA-AAM, the main peak at 987 cm^{-1} before the acid resistance test was shifted to 987, 1028 and 1023 cm^{-1} after 7, 14 and 28 days, respectively. For the outer surface of the LW-BP-AAM samples (Figure 8b), the main peak at 982 cm^{-1} before the acid resistance test was shifted to 1052, 1055 and 1055 cm^{-1} after 7, 14 and 28 days, respectively. For the centre part of the LW-BP-AAM before the acid resistance test, the main peak at 983 cm^{-1} was shifted to 1024, 1025 and 1010 cm^{-1} after 7, 14 and 28 days, respectively. The increase in this band indicates the removal of O-Al bond, which is less stable than the Si-O bond [25] and it can be verified by the apparently unchanged peak near ~776 cm^{-1}, which is corresponding to the Si-O-Si symmetric vibration [22] of of both FA-AAM and LW-BP-AAM in all tests. The vibration at ~1640 cm^{-1} and ~3440 cm^{-1} is assigned to the vibrations of hydroxyl groups O-H, due to the water contained in the sample [26].

3.3. Thermal conductivity

The coefficient of thermal conductivity of LW-BP-AAM with density around 1,100 kg/m^3 was 0.112 W/m·K which was much better in thermal performance in other reports that the coefficient of thermal conductivity of lightweight metakaolin/marble powder based geopolymer with EPS aggregates was 0.121 W/m·K at density about 500 kg/m^3 [18] and 0.47 W/m·K at density about 1,300 kg/m^3 [27] and 0.22 W/m·K at density about 600 kg/m^3 [19].

4. Conclusions

In this study, a new way to utilise the brick and XPS from CDW to form lightweight alkali activated material was investigated. The pre-treatment of raw materials from CDW to the precursor of alkali activated material, alkali activating solution and mixing procedure was discussed. From the

Preprints (www.preprints.org) | NOT PEER-REVIEWED | Posted: 25 June 2018 doi:10.20944/preprints201806.0387.v1

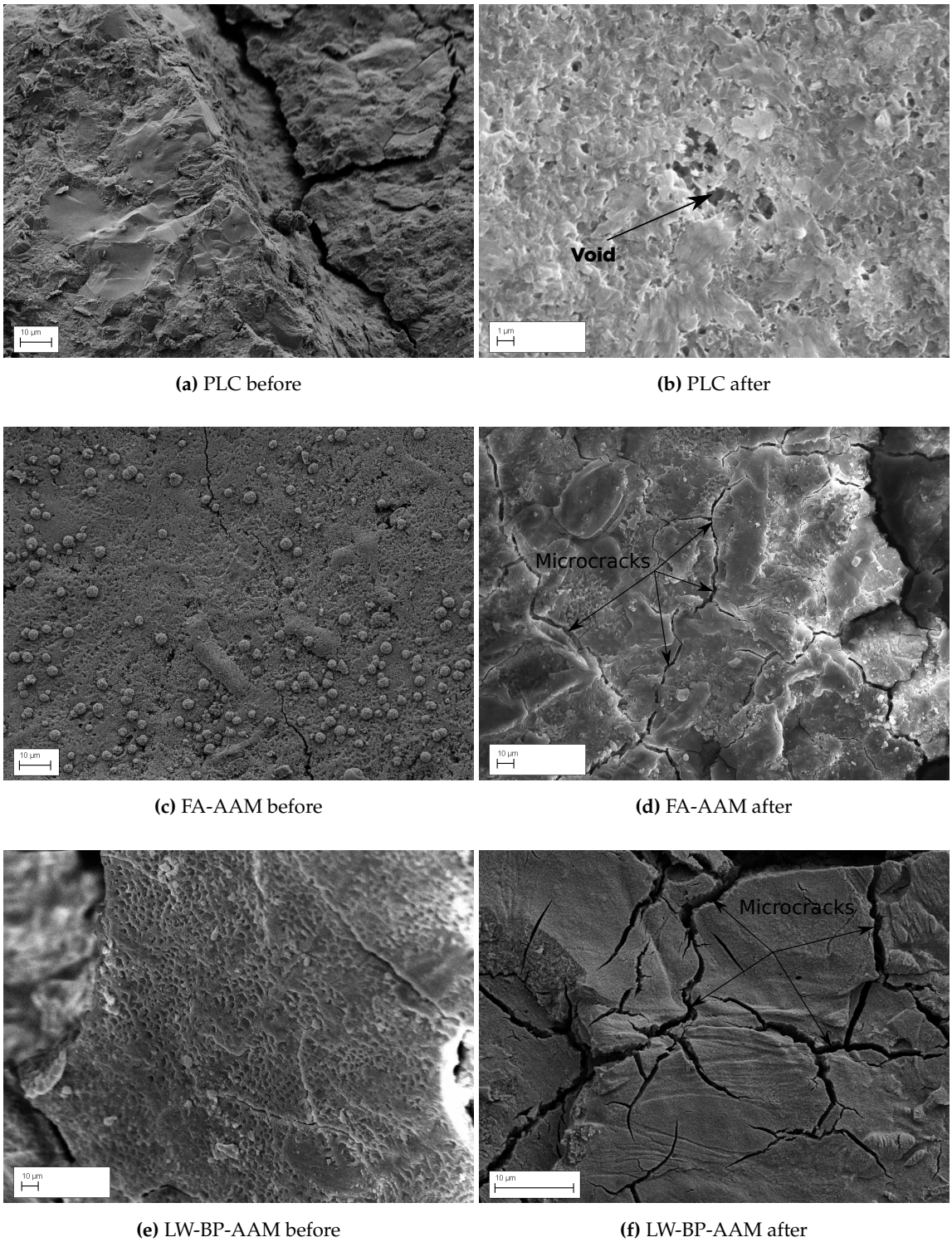

(a) PLC before **(b)** PLC after

(c) FA-AAM before **(d)** FA-AAM after

(e) LW-BP-AAM before **(f)** LW-BP-AAM after

Figure 7. Micrographs of PLC, FA-AAM and LW-BP-AAM before and after the acid test.

Preprints (www.preprints.org) | NOT PEER-REVIEWED | Posted: 25 June 2018 doi:10.20944/preprints201806.0387.v1

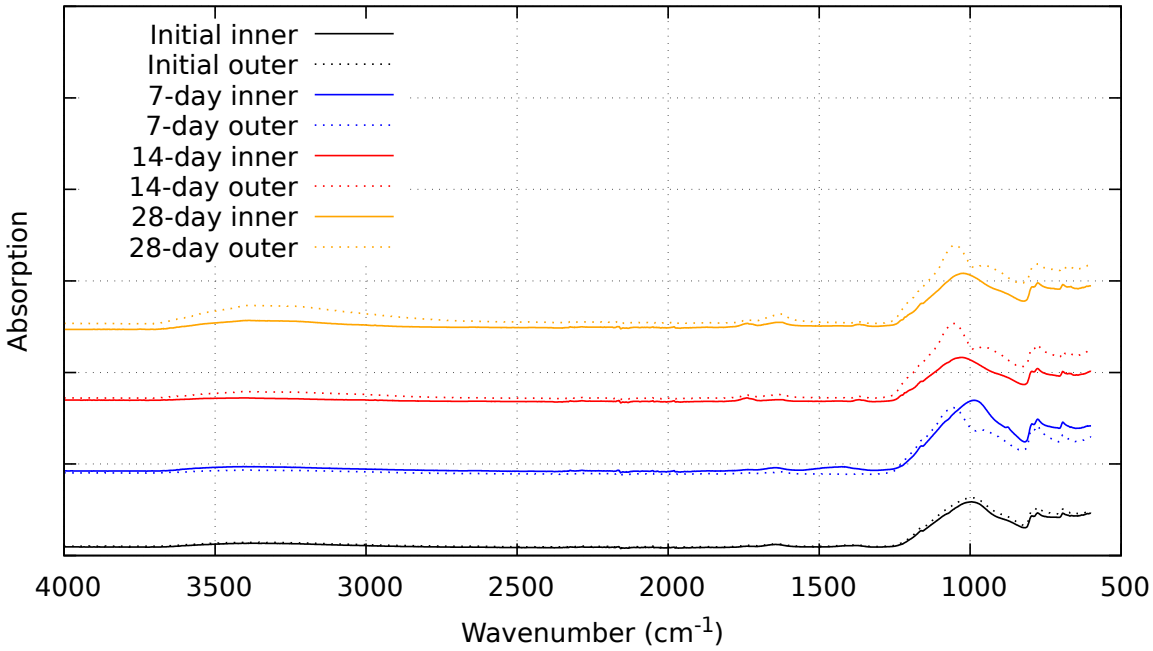

(a) FA-AAM

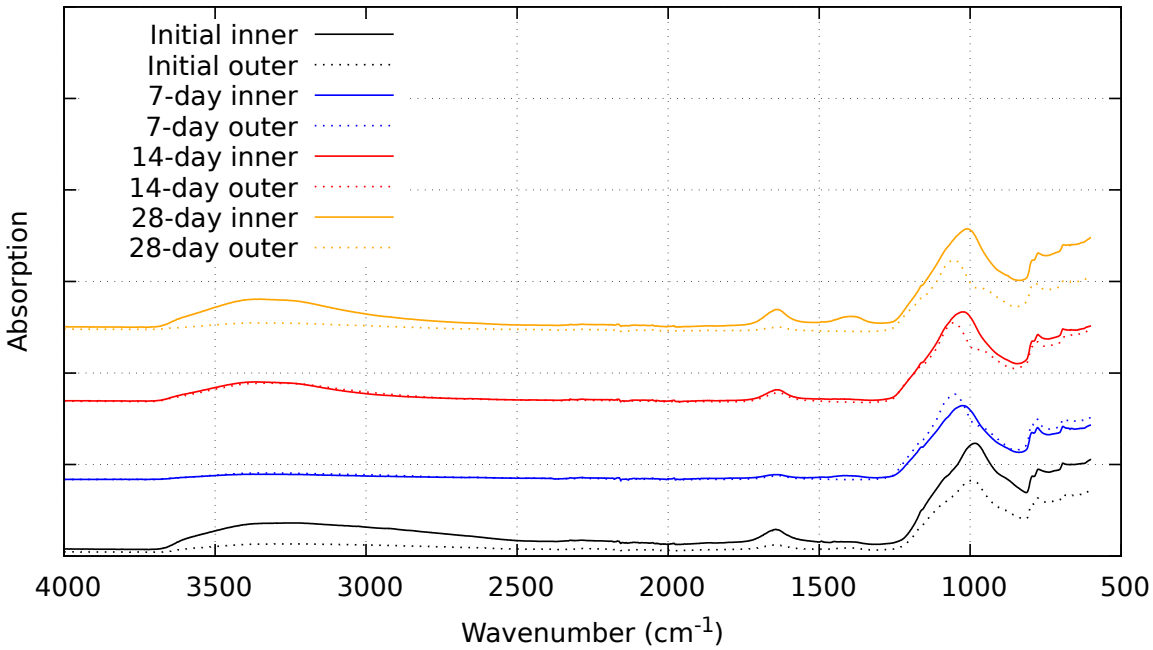

(b) LW-BP-AAM

Figure 8. FTIR spectra of (a) FA-AAM and (b) LW-BP-AAM.

inspection of acid resistance test, the stability of the proposed material was superior than Portland cement and comparable with conventional fly ash based alkali activated material. Although the compressive strength was not high compared the counterpart with EPS as the lightweight aggregates but it was better than counterpart by aeration. In all cases, the coefficient of thermal conductivity of the proposed material was lower than the material with similar range of density. The proposed material has brick-like appearance and it provides an alternative to make brick from CDW for non-structural applications.

Author Contributions: Conceptualization: Kai Tai Wan and Xiangming Zhou; Methodology: Kai Tai Wan; Validation, Kai Tai Wan, Gediminas Kastiukas and Xiangming Zhou; Formal Analysis: Kai Tai Wan; Investigation: Amende Sivanathan; Resources, Gediminas Kastiukas; Data Curation: Kai Tai Wan; Writing—Original Draft Preparation: Kai Tai Wan; Writing—Review & Editing: Kai Tai Wan; Visualization: Kai Tai Wan; Supervision: Kai Tai Wan and Xiangming Zhou; Project Administration: Gediminas Kastiukas; Funding Acquisition: Xiangming Zhou.

Funding: This research was funded by European Union's Horizon 2020 research and innovation programme under the Nanotechnologies, Advanced Materials, Biotechnology and Advanced Manufacturing and Processing (EEB-04-2016) grant agreement No 723825.

Acknowledgments: In this section you can acknowledge any support given which is not covered by the author contribution or funding sections. This may include administrative and technical support, or donations in kind (e.g. materials used for experiments).

Conflicts of Interest: The authors declare no conflict of interest.

Abbreviations

The following abbreviations are used in this manuscript:

XPS	extruded polystyrene
PLC	Portland-Limestone cement
FA	fly ash
FA-AAM	fly ash based alkali activated mortar
BP-CDW	brick powder from construction and demolition waste
BP-CDW-M	milled BP-CDW
LW-BP-AAM	lightweight BP-CDW-M based alkali activated mortar
AAS-FA	alkali activating solution for FA-AAM
AAS-BP	alkali activating solution for LW-BP-CDW-M-AAM
SSD	saturated surface dry
SEM	Scanning electron microscopy
EDX	energy dispersive X-ray spectroscopy
FTIR	Fourier transform infrared spectroscopy

References

1. Fischer, C.; Werge, M. *EU as a recycling society. In European Topic Centre on Resource Waste Management Working Paper 2/2009*; European Topic Centre on Sustainable Consumption and Production: Copenhagen, Denmark, 2009.
2. De Belie, N.; Robeyst, N. *Recycling of construction materials. In Environment-Conscious Construction Materials and Systems, State of the Art Report of TC 192-ECM. RILEM Report Nr. 37*; RILEM Publications S.A.R.L.: Bagneux, France, 2007.
3. Aliabdo, A.A.; Abd-Elmoaty, A..M.; Hassan, H.H. Utilization of crushed clay brick in concrete industry. *Alexandria Engineering Journal* **2014**, *53*, 151–168.
4. Kumar, M.; Chandramauli, A.; Ashutosh. Partial replacement of fine aggregates of fire bricks with fine aggregates in concrete. *International Journal of Civil Engineering and Technology* **2018**, *9*, 961–968.
5. Grabois, T.M.; Cordeiro, G.C.; Toledo Filho, R.D. *Hydration properties of cement pastes with recycled demolition waste from clay bricks and concrete*; Vol. 10, *RILEM Bookseries*, 2015.
6. Kırgız, M.S. Fresh and hardened properties of green binder concrete containing marble powder and brick powder. *European Journal of Environmental and Civil Engineering* **2016**, *20*, s64–s101.

7. Zhu, P.; Mao, X.; Qu, W.; Li, Z.; Ma, Z.J. Investigation of using recycled powder from waste of clay bricks and cement solids in reactive powder concrete. *Construction and Building Materials* **2016**, *113*, 246–254.
8. Pathak, A.; Kumar, S.; Jha, V.K. Development of Building Material from Geopolymerization of Construction and Demolition Waste (CDW). *Transactions of the Indian Ceramic Society* **2014**, *73*, 133–137.
9. Komnitsas, K.; Zaharaki, D.; Vlachou, A.; Bartzas, G.; Galetakis, M. Effect of synthesis parameters on the quality of construction and demolition wastes (CDW) geopolymers. *Advanced Powder Technology* **2015**, *26*, 368–376.
10. Greeley, T.R. A review of Expanded Polystyrene (EPS) properties, performance and new applications. *ASTM Special Technical Publication* **1997**, *1320*, 224–239.
11. Herki, B.A.; Khatib, J.M. Valorisation of waste expanded polystyrene in concrete using a novel recycling technique. *European Journal of Environmental and Civil Engineering* **2017**, *21*, 1384–1402.
12. Vakhshouri, B.; Nejadi, S. Size effect and age factor in mechanical properties of BST Light Weight Concrete. *Construction and Building Materials* **2018**, *177*, 63–71.
13. Feng, D.; Provis, J.L.; Van Deventer, J.S.J. Thermal activation of albite for the synthesis of one-part mix geopolymers. *Journal of the American Ceramic Society* **2012**, *95*, 565–572.
14. Ke, X.; Bernal, S.A.; Ye, N.; Provis, J.L.; Yang, J. One-part geopolymers based on thermally treated red Mud/NaOH blends. *Journal of the American Ceramic Society* **2015**, *98*, 5–11.
15. Subathra Devi, V. Durability properties of multiple blended concrete. *Construction and Building Materials* **2018**, *179*, 649–660.
16. Zhang, W.; Yao, X.; Yang, T.; Liu, C.; Zhang, Z. Increasing mechanical strength and acid resistance of geopolymers by incorporating different siliceous materials. *Construction and Building Materials* **2018**, *175*, 411–421.
17. British Standards Institution. *BS EN 196-1:2005 Methods of testing cement. Determination of strength*; BSI, 2005; pp. 1–36.
18. Colangelo, F.; Roviello, G.; Ricciotti, L.; Ferrándiz-Mas, V.; Messina, F.; Ferone, C.; Tarallo, O.; Cioffi, R.; Cheeseman, C. Mechanical and thermal properties of lightweight geopolymer composites. *Cement and Concrete Composites* **2018**, *86*, 266–272. doi:10.1016/j.cemconcomp.2017.11.016.
19. Zhang, Z.; Provis, J.; Reid, A.; Wang, H. Geopolymer foam concrete: An emerging material for sustainable construction. *Construction and Building Materials* **2014**, *56*, 113–127.
20. Sanjayan, J.G.; Nazari, A.; Chen, L.; Nguyen, G.H. Physical and mechanical properties of lightweight aerated geopolymer. *Construction and Building Materials* **2015**, *79*, 236–244.
21. Zhang, M.; Zhao, M.; Zhang, G.; Mann, D.; Lumsden, K.; Tao, M. Durability of red mud-fly ash based geopolymer and leaching behavior of heavy metals in sulfuric acid solutions and deionized water. *Construction and Building Materials* **2016**, *124*, 373–382.
22. Vempati, R.; Rao, A.; Hess, T.; Cocke, D.; Lauer, H. Fractionation and characterization of Texas lignite class 'F' fly ash by XRD, TGA, FTIR, and SFM. *Cement and Concrete Research* **1994**, *24*, 1153–1164. doi:10.1016/0008-8846(94)90039-6.
23. Handke, M.; Mozgawa, W. Model quasi-molecule Si2O as an approach in the IR spectra description glassy and crystalline framework silicates. *Journal of Molecular Structure* **1995**, *348*, 341–344. Molecular Spectroscopy and Molecular Structure 1994, doi:10.1016/0022-2860(95)08658-I.
24. Zhang, Z.; Wang, H.; Provis, J.L.; Bullen, F.; Reid, A.; Zhu, Y. Quantitative kinetic and structural analysis of geopolymers. Part 1. The activation of metakaolin with sodium hydroxide. *Thermochimica Acta* **2012**, *539*, 23–33. doi:10.1016/j.tca.2012.03.021.
25. Zhang, X.; Cheng, F. Comparative assessment of external and internal thermal insulation for energy conservation of intermittently air-conditioned buildings. *Journal of Building Physics* **2018**. Article in Press.
26. Ma, X.; Zhang, Z.; Wang, A. The transition of fly ash-based geopolymer gels into ordered structures and the effect on the compressive strength. *Construction and Building Materials* **2016**, *104*, 25–33. doi:10.1016/j.conbuildmat.2015.12.049.
27. Liu, M.Y.J.; Alengaram, U.J.; Jumaat, M.Z.; Mo, K.H. Evaluation of thermal conductivity, mechanical and transport properties of lightweight aggregate foamed geopolymer concrete. *Energy and Buildings* **2014**, *72*, 238–245.